ORIGINAL PAPER

Seasonal variations in water flux compositions controlled by leaf development: isotopic insights at the canopy–atmosphere interface

Pei Wang[1] · Haitao Sun[1] · Xiao-Yan Li[1] · Xin Song[2] · Xiaofan Yang[1] · Xiuchen Wu[1] · Xia Hu[1] · Hongyun Yao[1] · Jingjing Ma[1] · Juanjuan Ma[1]

Abstract

Water-stable isotopes provide a valuable tool for tracing plant-water interactions, particularly evapotranspiration (ET) partitioning and leaf water dynamics at the plant-atmosphere interface. However, process-based investigations of plant/leaf development and the associated isotopic dynamics of water fluxes involving isotope enrichment at plant-atmosphere interfaces at the ecosystem scale remain challenging. In this study, in situ isotopic measurements and tracer-aided models were used to study the dynamic interactions between vegetation growth and the isotopic dynamics of water fluxes (ET, soil evaporation, and transpiration) involving isotope enrichment in canopy leaves in a multispecies grassland ecosystem. The day-to-day variations in the isotopic compositions of ET flux were mainly controlled by plant growth, which could be explained by the significant logarithmic relationship determined between the leaf area index and transpiration fraction. Leaf development promoted a significant increase in the isotopic composition of ET and led to a slight decrease in the isotopic composition of water in canopy leaves. The transpiration (evaporation) isoflux acted to increase (decrease) the $\delta^{18}O$ of water vapor, and the total isoflux impacts depended on the seasonal tradeoffs between transpiration and evaporation. The isotopic evidence in ET fluxes demonstrates the biotic controls on day-to-day variations in water/energy flux partitioning through transpiration activity. This study emphasizes that stable isotopes of hydrogen and oxygen are effective tools for quantitative evaluations of the hydrological component partitioning of ecosystems and plant-climate interactions.

Keywords Water-stable isotopes · Water flux composition · Seasonality · Canopy leaves · Grassland ecosystem · Isotope tracer

Highlights
- Leaf development controlled the isotopic seasonal variations in water fluxes by regulating flux composition
- Leaf development slightly decreased the isotopic enrichment of canopy leaves
- Transpiration/evaporation acted to increase/decrease the $\delta^{18}O$ of water vapor, which actually affected by the seasonal trade-off between them

✉ Pei Wang
  peiwang@bnu.edu.cn

1 State Key Laboratory of Earth Surface Processes and Resource Ecology, Faculty of Geographical Science, Beijing Normal University, Beijing 100875, China

2 College of Life Sciences and Oceanography, Shenzhen University, 3688 Nanshan Avenue, Shenzhen 518000, Guangdong, China

Introduction

Stable isotopes of water (δ^2H and $\delta^{18}O$) provide effective tools for tracing water fluxes within the soil–plant–atmosphere continuum (SPAC) and have been widely used for evapotranspiration (ET) partitioning (Moreira et al. 1997; Yepez et al. 2003; Williams et al. 2004; Wang et al. 2010; Wang et al. 2015; Xiao et al. 2018), as well as investigating the dynamics of water exchange at the interfaces (e.g., ground soil surfaces and leaf surfaces) between the land surface and atmosphere (Dongmann et al. 1974; Farquhar and Cernusak 2005; Lai et al. 2005; Cernusak et al. 2016). Plant transpiration (T) is the largest component of the terrestrial-atmospheric water/energy flux, accounting for somewhere between 50 and 90% of the annual global land surface water flux (Good et al. 2015; Jasechko et al. 2013; Maxwell and Condon 2016; Lian et al. 2018). Therefore, vegetation exerts strong feedback effects on the climate by modifying the energy, momentum, and hydrologic balances of the land surface (Twine et al.

2000; Arora 2002; Fatichi et al. 2016). Climatic feedback effects resulting from vegetation are mainly attributable to the physiological properties of vegetation, such as the leaf area index (LAI), stomatal resistance, rooting depth, albedo, and surface roughness and its effect on soil moisture (Arora 2002). The seasonal rhythm of ecosystem transpiration emerges from interactions among the climate, plant functional traits, and ecosystem structure. An increasing number of studies report a close relationship between the LAI and transpiration fraction (T/ET), indicating that leaf development dominates the water flux composition (e.g., Hu et al. 2009; Wang and Yamanaka 2014; Wang et al. 2014; Wei et al. 2015, 2017; Wang et al. 2018b). Higher correlations between the LAI and evapotranspiration ratio, $lET/(R_n - G)$, where lET is the latent heat flux, R_n is the net radiation, and G is the ground heat flux, were also reported, illustrating that the energy flux composition is largely regulated by plant growth (e.g., Wilson et al. 2002; Li et al. 2005; Hammerle et al. 2008, Zhao et al. 2017). However, few isotopic investigations within the SPAC have been conducted to improve the understanding of the interactions between plant/leaf development and the isotopic dynamics of water fluxes (ET, T, and soil evaporation, E) along with the isotopic dynamics at the plant-atmosphere interface. In addition, the biophysical effects of vegetation on the climate have been addressed in a number of studies investigating the effects of deforestation or clear-cutting (Charney 1975; Dickinson and Henderson-Sellers 1988; Lean and Rowntree 1997; Zhou et al. 2015), while only a few investigations have been conducted to examine the biophysical effects of mowing from a water-isotopic perspective in grassland ecosystems.

The isotopic composition of ET (δ_{ET}) provides valuable information for tracing the atmospheric water cycle (e.g., water sources and flow paths) and for diagnosing plant activities and their roles in the hydrological cycle. Currently, indirect techniques, including the Keeling plot approach (Good et al. 2014; Keeling 1958; Yakir and Wang 1996; Wang et al. 2010), flux-gradient method (Good et al. 2012; Hu et al. 2014; Wen et al. 2016; Wang et al. 2016), and direct eddy covariance measurements (Jelka et al. 2019), are widely used for estimating δ_{ET}. As is clear, the isotopic composition of water vapor (δ_V) is an essential variable that must be determined to derive δ_{ET} using the abovementioned methods. The traditional cold-trap methods for measuring δ_V are accurate but suffer from coarse time resolutions (Yakir and Wang 1996; Yakir and Sternberg 2000). Rapid developments in laser techniques have largely overcome this methodological constraint by enabling the online, near-continuous quantification of water vapor isotopes and, by extension, δ_{ET} (Lee et al. 2005, Wen et al. 2008, Griffis 2013). However, the Keeling plot, gradient-based, and eddy covariance methods also involve many uncertainties (Good et al. 2012) and sometimes fail to reflect the true values of δ_{ET}, particularly during periods of poor information retrieval or top-down diffusion (entrainment, which represents another end member). Nevertheless, these approaches focus on the measurement of δ_{ET}, which lacks crucial

information on the components of ET, hindering our understanding and ability to trace water transfers through the SPAC. The term δ_{ET} represents the comprehensive result of the interactions among the climate, soil, and biosphere. Many land-surface models with isotopic tracers have been established (e.g., Braud et al. 2005; Henderson-Sellers et al. 2006; Riley et al. 2002; Yoshimura et al. 2006; Xiao et al. 2010). To date, there are still many challenges involved in capturing the isotopic signals of soil evaporation, transpiration, and their mixing process (Griffis 2013). The SPAC model is relatively simple but is still capable of incorporating separate water/energy controls on vegetation and soil as well as coupling isotopic fractionation with H_2O exchange and the mixing processes in terrestrial ecosystems (Wang et al. 2016).

Isotopic variations in water fluxes and the isotopic enrichment process at the plant-atmosphere interface involve many factors that occur simultaneously but are usually studied in isolation (e.g., Wang et al. 2010; Xiao et al. 2012; Wen et al. 2016). Many models exist for simulating the isotopic composition of bulk leaf water ($\delta_{L,b}$), such as the isotopic steady-state (ISS) model (Craig and Gordon 1965), the non-steady-state (NSS) model (Dongmann et al. 1974; Helliker and Ehleringer 2000; Cernusak et al. 2003; Barbour et al. 2000, 2004), and the NSS model with the Péclet effect (Farquhar and Cernusak 2005)). Additionally, simple two-pool mixing models (Leaney et al. 1985; Song et al. 2015) and models based on the Péclet effect (Farquhar et al. 1993; Cuntz et al. 2007) have been used to simulate $\delta_{L,b}$ and the isotopic distribution within a single leaf. Although many studies have been conducted to evaluate these models under natural conditions (Barnard et al. 2007; Kahmen et al. 2008; Xiao et al. 2012; Dubbert et al. 2014), only a few studies have included model-measurement comparisons for δ_{ET} and $\delta_{L,b}$ at an ecosystem scale (Lee et al. 2007; Xiao et al. 2010). To date, comprehensive investigations of the isotopic dynamics of water fluxes (ET, T, and E) along with isotopic enrichment processes at the plant-atmosphere interface are still missing.

Land-surface models are promising tools for integrating isotopic fractionation processes with separate E and T in terrestrial ecosystems and have the advantages of long-term assessments of ET partitioning (Wang et al. 2015, 2016; Wei et al. 2018b) and isotopic enrichment at vegetation/soil-atmosphere interfaces across multiple temporal scales (Sprenger et al. 2016; Dubbert and Werner 2019; Wang et al. 2018a). Isotopic measurements (e.g., the Keeling plot and gradient-based approaches for δ_{ET}, field sampling with vacuum extractions of leaf water in the laboratory to obtain $\delta_{L,b}$) combined with modeling approaches have been demonstrated to be reliable in most cases (Wei et al. 2018a). In this study, isotopic measurements of various water pools (e.g., soil, plants, and the atmosphere) are combined with an isotope-enabled SPAC model (Iso-SPAC) to assess the seasonality of the isotopic compositions of soil evaporation (δ_E),

transpiration (δ_T), evapotranspiration (δ_{ET}), and bulk leaf water ($\delta_{L,b}$) and their relations with vegetation dynamics (e.g., LAI development). The objectives of the present study were to (1) evaluate the seasonality of the isotope compositions of water fluxes (δ_{ET}, δ_T, and δ_E) and bulk leaf water ($\delta_{L,b}$) in a grassland ecosystem and (2) investigate the factors controlling seasonal variations in δ_{ET}.

Materials and methods

Study site

We conducted field investigations at the Center for Research in Isotopes and Environmental Dynamics (CRiED) experimental site at the University of Tsukuba, Japan (36.1° N, 140.1° E), 27 m above sea level. Based on the observations collected between 1981 and 2005 at this site, the mean annual air temperature and the mean annual precipitation were approximately 14.1 °C and 1159 mm, respectively. The dominant plant species are *Solidago altssaima*, *Miscanthus sinensis*, and *Imperata cylindrical*. The study site, a flat circular field with a diameter of 160 m, is surrounded by pine forests and lawns. Mowing was performed on DOY 213 and 214 (August 1st and 2nd) in 2011. The soil surface was covered by litter made up of mown and dead plants from previous years. The top of the soil consists of a rich volcanic ash layer approximately 2 m thick, underlain by a clay layer.

Continuous micrometeorological and eddy covariance measurements of plant dynamics

Routine micrometeorological (e.g., downward solar radiation, air temperature, relative humidity, wind speed, and soil heat flux) and eddy covariance measurements (sensible heat flux and latent heat flux) were conducted in the CRiED experimental fields (Hiyama et al. 1993). More details of the instruments and the database used in this study are described in Ma et al. (2018). The fresh grass leaves from three randomly selected 1*1 m quadrats were harvested and LAI was measured by an automatic area meter in laboratory (AAM-7, Hayashi Denko, Tokyo, Japan) every week or every other week. In the periods without measurements, the LAI values were estimated by curve fitting: before mowing, LAI = 3.97 ln (DOY) - 18.70 (R^2 = 0.99), and after mowing, LAI = 6.15 ln (DOY) - 32.85 (R^2 = 0.95). At the same time, the total leaf water weight per unit ground surface (W, kg m^{-2}) was measured by weighing fresh and dried leaves before and after the LAI measurements, respectively, were conducted on each day. The vegetation height (Zp) was measured every 7 to 15 days throughout the study period. A close relationship was found between the LAI and W, with a linear function of W = 320.0 LAI – 46.05 (R^2 = 0.93).

Isotopic measurements

Field investigations of various water pools (water vapor, soil water, plant stem water, and leaf water) were conducted between April and September 2011. The isotopic measurements of water vapor were conducted by the traditional cold-trap method during the period from mid-day to early afternoon (1300–1500 JST) every week for laboratory analysis. The water vapor sampling system used in this study was described by Yamanaka and Tsunakawa (2007). The isotopic sampling of atmospheric water vapor combined with air temperature and air humidity measurements were conducted at three levels, and the sampling heights were adjusted with the development of canopy. In the early growing season (DOY 117~DOY 124) and a period after mowing (DOY 215~DOY 236), the three sampling heights were 160 cm, 50 cm, and 5 cm, respectively. In the rapid growing season, the three sampling heights were 200 cm, 70 cm, and 5 cm, respectively. At the same time, leaf water, stem water, and soil water samples were collected. Leaf samples from different species (*Solidago altssaima*, *Miscanthus sinensis*, and *Imperata cylindrica*) were collected separately. Leaf and stem water samples were extracted in triplicate in the laboratory by cryogenic vacuum distillation (Dawson and Ehleringer 1993; West et al. 2006). Soil water samples were collected at five depths (5 cm, 10 cm, 20 cm, 40 cm, and 80 cm) on each sampling day using suction lysimeters with ceramic cups attached on their tips (DIK-8390, Daiki, Japan) and 100-ml syringes (Zhao et al. 2013). Precipitation samples were collected every 2–3 days using a high-density polyethylene tank with a funnel.

The isotopic ratios of the water samples were analyzed at the CRiED. The hydrogen and oxygen stable isotopic compositions of the water samples were determined using a liquid water isotope analyzer (L1102-i, Picarro, Santa Clara, CA, USA). The isotopic ratios of $^{18}O/^{16}O$ and D/H were expressed as $\delta^{18}O$ and δD, respectively, relative to Vienna Standard Mean Ocean Water. The analytical errors were 0.1‰ for $\delta^{18}O$ and 1‰ for δD (Yamanaka and Onda 2011).

Processed-based modeling approach

The Iso-SPAC model developed by Wang et al. (2015) was used in this study, and the details of the model and relevant equations are provided in Method S1. Briefly, Iso-SPAC is an energy-balanced two-source model (soil surface and canopy interface) used to simulate day-to-day energy (R_n, lET, H, and G), ET, E, and T fluxes (Wang and Yamanaka 2014). Based on the outputs of resistance, surface temperature, and water fluxes at the soil surface and canopy interface, an isotopic budget is coupled by integrating the isotopic fractionation processes with E and T processes. This model was selected for several reasons. First, this model treats water fluxes and the isotopic compositions of plant transpiration and soil

evaporation separately and simultaneously integrates them to determine the isotopic composition of the ET flux. Second, the Iso-SPAC model, which includes three submodels with a range of complexities, namely, the ISS (Craig and Gordon 1965), NSS-D74 (Dongmann et al. 1974), and NSS-F05 (Farquhar and Cernusak 2005), was previously used at the leaf scale. The submodules were adopted here for the $\delta_{L,b}$ and δ_T determinations. The Iso-SPAC model can be validated not only by physical components (e.g., ET, T, E, leaf temperature, and energy flux) but also by isotopic components (δ_{ET}, δ_T, δ_E, $\delta_{L,b}$), which are expected to be more robust and reliable. Third, the radiation/energy balances in both the vegetative canopy and at the ground surface were solved by the Newton-Raphson scheme, enabling us to estimate the vegetation canopy temperature (T_L) and ground temperature (T_G) separately. The scheme can easily integrate isotopic fractionation processes with H_2O exchanges, and it has the advantage of enabling the long-term assessment of ET compositions as well as isotopic enrichment at the plant-atmosphere interface. Based on biophysical measurements (e.g., radiation, air temperature, humidity, LAI) and field observations of the isotopic compositions of soil water, stem water, and water vapor, the Iso-SPAC model can output the seasonal variations in δ_T, δ_E, δ_{ET}, and $\delta_{L,b}$ (Table S1). The root mean square error (RMSD), the I index (Willmott et al. 1985), and R^2 (R is the correlation coefficient) were used to evaluate the model performance.

Determination of the transpiration fraction and evapotranspiration ratio

The transpiration fraction (T/ET) was determined by both the Iso-SPAC model (Method S1, heat and water flux part of the Iso-SPAC model) and by direct isotope measurements (Method S2). The evapotranspiration ratio (lET/(R_n – G)) was determined by both eddy covariance system measurements in the field and simulations using the Iso-SPAC model (Method S1).

Results

Observed seasonal variations in meteorology, flux, and leaf development

The air temperature increased progressively from DOY 110 to DOY 213, with a marked increase after grass cutting occurred during DOY 213–214, and then decreased gradually. The relative humidity exhibited much larger variations, with an obvious decrease after grass cutting (Fig. 1a). Table 1 summarizes the observed monthly meteorological factors. The latent heat flux (lET) dominated the energy flux during the growing season. With grass cutting, the lET dropped sharply, and the sensible heat flux (H) increased correspondingly, which

illustrated that vegetation growth has obvious effects on energy flux partitioning (Fig. 1b). The observed seasonal variations in volumetric soil water and the LAI are shown in Fig. 1c. The soil water content (0–20 cm) varied substantially during the growing season. The mean LAI increased from 0.16 to
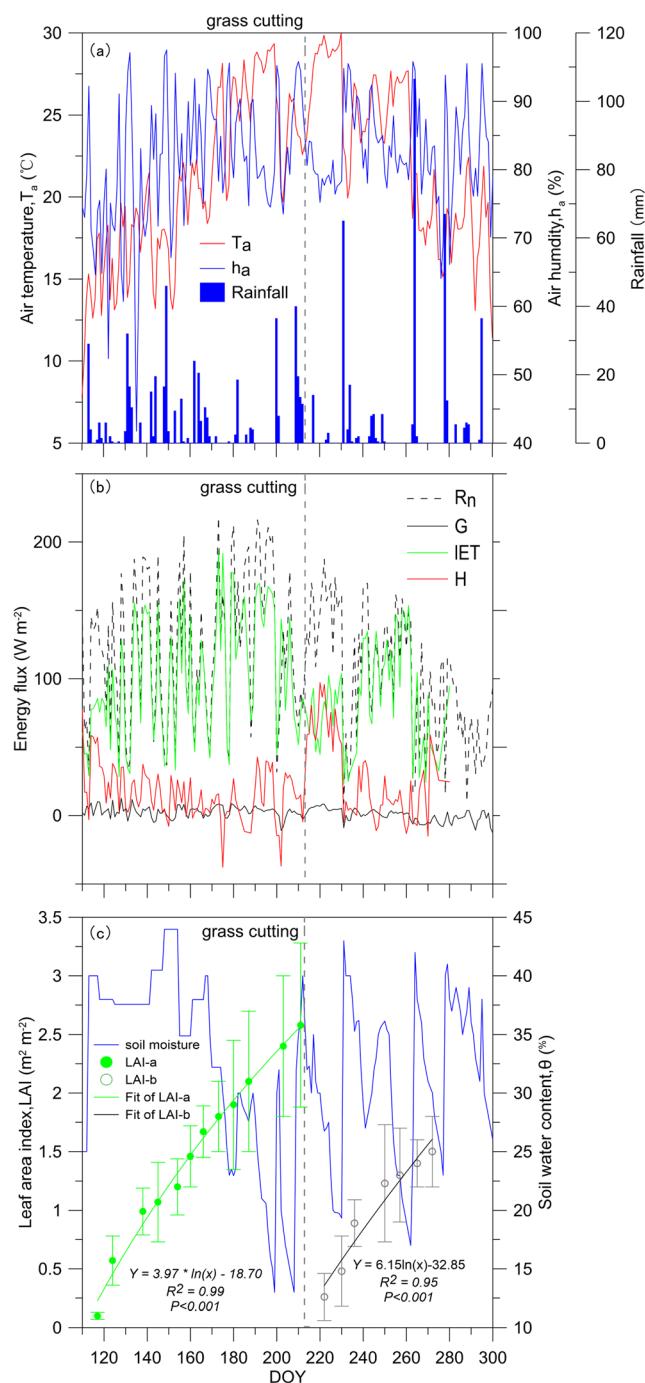

Fig. 1 Seasonal variations in the (**a**) air temperature (T_a) and relative humidity (h_a); (**b**) energy fluxes (net radiation (R_n), sensible heat flux (H), latent heat flux (lET), and ground heat flux (G)) measured by the EC system; and (**c**) volumetric soil water (%) and leaf area index (LAI). LAI-a and LAI-b represent the stages of plant growth before and after grass cutting. Dotted gray lines show the days of mowing

Month	^aT_a (°C)	^bh_a (%)	Precipitation (mm)	Wind speed (m s^{-1})	^cLAI (m^2 m^{-2})	^dZ_p (m)
Apr 2011	13.70	73.88	113.18	1.06	0.16	0.01
May 2011	17.04	77.24	288.86	1.23	1.10	0.88
June 2011	21.31	84.07	13.64	0.71	1.84	1.72
July 2011	25.93	83.81	230.45	0.76	2.49	2.37
Aug 2011	26.25	83.35	73.64	0.80	0.76	0.50
Sep 2011	23.63	84.01	310.91	0.81	1.48	1.31
Oct 2011	17.77	81.26	102.27	0.78	2.06	1.97

Table 1 Summary of monthly meteorological and vegetation properties

^{a} Air temperature

^{b} Relative humidity

^{c} Leaf area index

^{d} Vegetation height

2.49 m^2 m^{-2} before grass cutting. After grass cutting, the plant LAI increased again from 0.76 to 2.06 m^2 m^{-2}.

Observed isotopic signatures of water pools and fluxes during the growing season

A dual isotope-based approach (δ^{18}O and δ^2H) was used to examine the linkages between various water pools and water fluxes. From April to October 2011, water isotopic signals were monitored in five soil layers, groundwater, plant leaves, and stems from three species, rainfall, and water vapor from three layers, and δ_{ET} was estimated by the Keeling plot approach for a grassland ecosystem (Fig. 2). The linear fits of δ^{18}O and δ^2H in

local rainfall were very close to the GMWL (global meteoric water line). The $\delta_{L,b}$ values for the three species showed a wide range of isotopic fractionation and high values due to transpiration. The isotopic signal of the stem water of each species was close to those of precipitation and deep soil water. The isotopic composition of surface soil water (5 cm) varied over time because of precipitation and evaporation. Fluctuations in deep soil water (20, 40, 60, and 80 cm) decreased with depth and remained small below 40 cm. The δ_V values at the three levels were similar and showed low isotopic values. The δ_{ET} values estimated by the Keeling plot approach varied from −10.71 (−65.55) to −20.24 (−137.18) ‰ for ^{18}O/^{16}O (D/H) during the growing season; these results are summarized in Method S2.
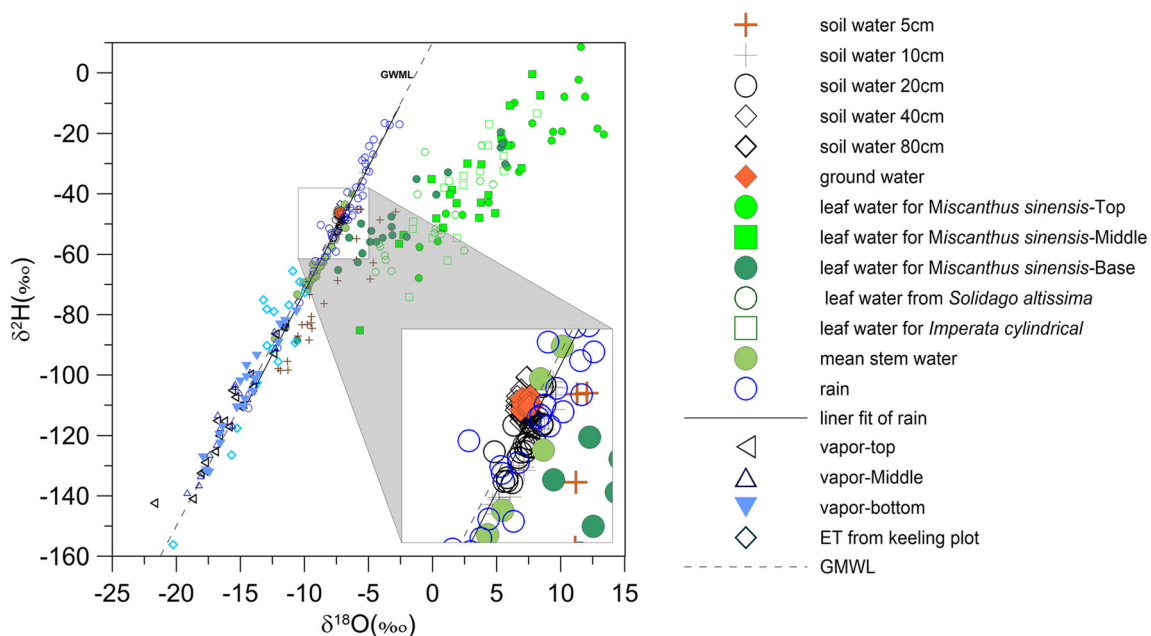

Fig. 2 Dual-isotope plot for all samples (soil water, groundwater, plant leaf and stem water, rainfall, water vapor, and evapotranspiration) collected, analyzed, and estimated in a grassland ecosystem. Soil water collected from five layers (5cm, 10cm, 20cm, 40, 80cm). Leaf and stem water were collected from the top, middle, and base of *Miscanthus sinensis*, as well as the whole *Solidago altissima*, and *Imperata*

cylindrical. Water vapor collected from three heights, and isotope composition in evapotranspiration (ET) estimated by a Keeling plot approach. Isotopes were collected during the growing season, from DOY 110 to 300. GMWL is the global meteoric water line (solid line, δ^2H=10 + 8 δ^{18}O). The dashed line is a linear fit of all rainfall samples collected during the growing season (dashed line, δ^2H=10.2 + 8.2 δ^{18}O)

Model performance

The model performance in representing energy fluxes, leaf temperature, and canopy conductance is summarized in Table S2. Very good agreement between the observations and models can be found for all energy fluxes, with small RMSD (14.7–36.8 W m^{-2}) values and high I indices (0.56–0.92). Similar results were obtained for the canopy leaf temperature and leaf stomatal conductance, with RMSD values of 2.08 °C and 1.97 mm s^{-1} and I indices of 0.99 and 0.79, respectively. In addition, the model performances in a range of isotopic scenarios (e.g., ISS and NSS) can be assessed from the observed isotopic signatures (δ_{ET}, $\delta_{L,b}$). Field sampling and measurements of leaf-water isotopic compositions for each species and the representative canopy-scale bulk leaf water measurements are summarized in Table S3. The agreement between the measured (Table S3 and Table S4) and simulated values demonstrates the accuracy of the proposed model for reconstructing day-to-day variations in both δ_{ET} and $\delta_{L,b}$ (Table 2). Among the four submodules, ISS had the best performance in reconstructing day-to-day variations in δ_{ET} and $\delta_{L,b}$ at the ecosystem scale, with smaller RMSD (1.69 and 2.08, respectively) values and high I indices (0.91 and 0.40, respectively). The results illustrated that ISS can be used to obtain a reasonable assumption for the selected grassland ecosystem because of its fast transpiration and rapid turnover of water in leaves, resulting in a transpiration signature similar to that of the source water.

Reasonable agreement (R^2 =0.45 and 0.30 for transpiration fraction and evapotranspiration ratio, respectively) was obtained between the observed and modeled mean daily ratios of both the transpiration fraction (T/ET) and evapotranspiration ratio (lET/R_n – G) (Fig. 3). The modeled evapotranspiration ratio agreed reasonably well (R^2 =0.30) with the ratios observed by the EC system, but the modeled values were mostly underestimated when the measured ratio was over 0.7. The differences between the isotopic measurements and numerical simulations ranged from 1 to 26% during the growing season, with an average of 6%. Considering the uncertainty of isotope measurements, the reasonable

consistency between the two methods indicates the reliability of the water flux partitioning results. Therefore, it is expected that the partitioning results are robust and reliable for quantifying the water/energy flux components with high LAI (e.g., LAI >1) values. The simulated T (E) flux ranged from 0 to 7.24 mm day^{-1} (0 to 1.65 mm day^{-1}), with an average value of 2.05 ± 1.56 mm day^{-1} (0.52 ± 0.37 mm day^{-1}) during the growing season.

Temporal dynamics of the isotopic compositions of water fluxes and bulk leaf water

Figure 4 shows the seasonal variations in the LAI, δ_{ET}, δ_T, δ_E, and $\delta_{L,b}$ obtained by both field measurements and the Iso-SPAC model outputs. The δ_T values exhibited the smallest seasonal variations, whereas δ_E showed the largest variations. At the ecosystem scale, if the transpiration process was at an isotopic steady state (ISS) at a daily scale, then δ_T would equal that of the water used by plants (Flanagan et al. 1991). In contrast, the water evaporated from soil surfaces was strongly fractionated and depleted in heavy isotopes (Craig and Gordon 1965; Gat 1996). There was a significant difference between δ_T and δ_E. The day-to-day δ_{ET} values increased with leaf development, showed a marked decrease during grass cutting, and increased gradually with plant regrowth. The daily $\delta_{L,b}$ values decreased gradually with leaf development during the fast growing period and showed an increase after grass cutting.

Relationships between leaf development and the isotopic signatures of water fluxes and canopy leaf water

Figure 5a shows the relationship between the LAI and δ_{ET} obtained by Keeling plot measurements and the Iso-SPAC model output with ISS, which was chosen because of its superior performance. A good logarithmic relationship was found between the LAI and δ_{ET}, with an R^2 of 0.83 for the modeled dataset. The

Table 2 Model performance statistics for the isotope compositions of evapotranspiration flux (δ_{ET}) and bulk leaf water ($\delta_{L,b}$)

Variables	$\delta_{L,b}$				δ_{ET}		
$\delta^{18}O$ (δD)	ISS with two pools	ISS with Péclet effect	[a]NSS with two pools	NSS with Péclet effect	[b] ISS with two pools	NSS with two pools	NSS with Péclet effect
R^2	0.72 (0.62)	0.54 (0.55)	0.72 (0.61)	0.68 (0.61)	−(0.26)	−(0.26)	−(0.26)
I index	0.91 (0.80)	0.82 (0.74)	0.91 (0.80)	0.82 (0.63)	0.40 (0.41)	0.32 (0.41)	0.32 (0.47)
RMSD ‰	1.69 (13.25)	2.59 (16.71)	2.54 (11.91)	2.61 (22.92)	2.08 (21.68)	2.08 (21.68)	2.08 (21.68)
n	21	21	21	21	14	14	14

[a] Non-steady-state (NSS) model for isotope composition at evaporation site ($\delta_{L,e}$)

[b] Isotopic steady-state assumption (ISS) with two pools and ISS with the Péclet effect had the same performance for simulating δ_{ET}. Updated from Wang et al. (2015)
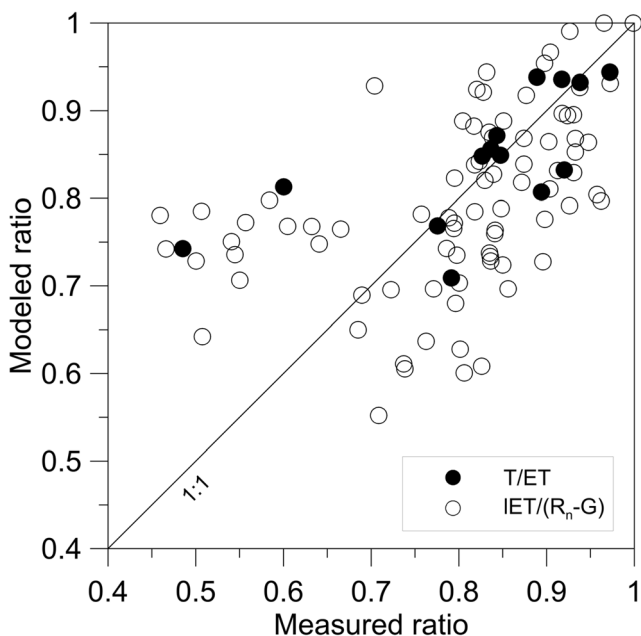
Fig. 3 Comparison of measured and modeled daily mean flux ratios; T is transpiration, ET is total evapotranspiration, lET is latent heat flux, R_n is net radiation, and G is soil heat flux
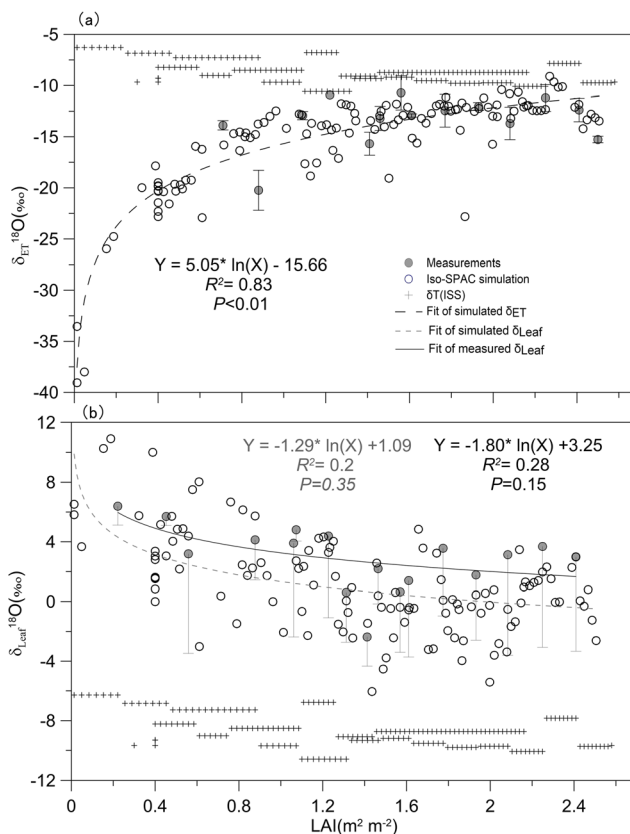

Fig. 5 Relationships between the leaf area index (LAI) and (**a**) the oxygen isotopic compositions of ET (δ_{ET}) obtained by both the Keeling plot approach and the simulation using the Iso-SPAC model incorporating an isotopic steady state (ISS) for the transpiration flux and (**b**) bulk leaf water ($\delta_{L,b}$) at the canopy scale obtained by field measurements and numerical modeling. The cross symbols represent the isotopic compositions of the transpiration flux (δ_T)

Keeling plot approach showed a similar relationship. Figure 5b shows the relationship between the LAI and isotopic signals of canopy leaf water ($\delta_{L,b}$) obtained from both field measurements and the Iso-SPAC model simulation. The field-measured $\delta_{L,b}$ had a similar but smaller slope compared with that of the Iso-SPAC model-simulated value, which may be caused by the coarse time resolution of the field-measured data. With leaf development, δ_{ET} gradually became enriched and approached δ_T (Fig. 5a), whereas $\delta_{L,b}$ lost isotopic enrichment (Fig. 5b). These results illustrate that leaf development greatly affects seasonal variations in δ_{ET} and $\delta_{L,b}$.

Fig. 4 Seasonal variations in the leaf area index (LAI), the oxygen isotopic composition of measured water vapor (δ_V), the evapotranspiration (δ_{ET}) values estimated by the Keeling plot approach and the Iso-SPAC model, and the oxygen isotopic compositions of transpiration (δ_T) and soil evaporation (δ_E) simulated by the Iso-SPAC model. The canopy-scale oxygen isotopic composition of bulk leaf water ($\delta_{L,b}$) was simulated by the Iso-SPAC model, and the measured $\delta_{L,b}$ values were obtained during the growing season. Error bars represent the standard deviations of the leaf samples within and among species

Discussion

Biotic control of seasonal variations in δ_{ET}

Identifying the factors that control δ_{ET} is vital for tracing the atmospheric water cycle. However, this remains a great challenge because δ_{ET} is interactively affected by multiple factors, including the climate (e.g., air temperature, relative humidity, wind speed, solar radiation, the isotopic compositions of rainfall, and water vapor), soil (e.g., soil moisture, the isotopic composition of soil water, soil texture, and temperature), and the biosphere (e.g., LAI, Z_p, canopy structure, the isotopic composition of source water used by plants). Combining isotopic measurements (e.g., Keeling plots, gradient-based approach) with a modeling approach for estimating δ_{ET} is more reliable than using a single approach in most cases (Wang et al. 2015). The agreement between the model simulations and observations demonstrates that using the Iso-SPAC model with ISS to determine T can reproduce reasonable day-to-day variations in all surface energy balance components, as well as δ_{ET}. Sensitivity analyses of both the physical flux part and the isotope part suggested that T/ET is relatively insensitive to uncertainties or errors in the assigned model parameters and measured input variables, which illustrates the robustness of flux partitioning (Wang et al. 2015). Few studies have investigated the dominant factors controlling δ_{ET}. The results obtained here reveal a good nonlinear relationship between the LAI and δ_{ET}, as obtained by both the Iso-SPAC simulation and Keeling plot measurements. As shown in Fig. 4, the isotopic composition of rainfall ($\delta_{rainfall}$) affects the δ_{ET} values through the regulation of soil water dynamics (e.g., the isotopic composition of soil water, δ_S) and plant uptake processes (e.g., the isotopic composition of stem water, δ_X). The δ_S and δ_X, terms, when used as origin sources during soil evaporation and transpiration analyses were well represented in Craig and Gordon (1965) as well as in ISS and non-steady state models (Method S1). Generally, dynamic variations in δ_{ET} can be explained by δ_E, δ_T and their mixing ratio (e.g., T/ET or E/ET) measured at daily intervals, as shown in Eq. S27. This study found that T/ET has a close relationship with the LAI (Fig. S1), but no significant relationship was found for δ_E and δ_T during the growing season (Fig. S2), which indicates that $\delta_{rainfall}$ has less of an effect on δ_{ET}. Therefore, the LAI exerts a dominant effect on the day-to-day variations in δ_{ET} within the lower (δ_E, range from −24.76 to −86.75‰) and upper (δ_T, range from −6.28 to −10.57‰) limits by controlling T/ET. Early in the growing season, δ_{ET} showed isotopic depletion, indicating that E dominated the total ET flux, and δ_{ET} was subsequently more affected by δ_E. With ongoing leaf development, both T/ET and lET/(R_n-G) increased, illustrating the increasing biotic control on the ecosystem water/energy flux partitioning (Fig. S1). As the LAI increased, more water was lost by T, and δ_{ET} became enriched due to the increased T and was consequently better reflected by δ_T.

Towards a better understanding of ecosystem behavior using isotopic tracers

Figure 6 shows a set of box-and-whisker plots presenting the minimum, maximum, median, lower quartile, and upper quartile of all water pools and fluxes in the studied temperate grassland ecosystem. The seasonal variations in the isotopic composition of soil water decreased in amplitude with soil depth. The δ_s value at a depth of 80 cm hardly showed any change. In contrast, the δ_s values at shallower depths varied over time with isotopic inputs from precipitation and soil evaporation. Under field conditions, the leaf-water isotopic composition showed large deviations both within and among species, even for single leaves (Table S3). For canopy leaf water, a previous study showed that the isotope fractionation factors acting at the leaf scale can behave differently at the canopy scale (Lee et al. 2009), and a distinction should be made between leaf- and canopy/ecosystem-scale processes. By incorporating the environmental conditions outside the plant community in the atmospheric surface layer, the appropriate modeling framework could be applied at the ecosystem scale, reflecting the community behavior and ecosystem properties. Therefore, despite the heterogeneity caused by the biodiversity and position of leaves, $\delta_{L,b}$ can be measured and predicted for multispecies grassland ecosystems at a daily time scale (Fig. 4). A comparison between the field measurements and the simulations performed by the four submodels indicated that ISS can be achieved at the ecosystem scale (Table 2). Isotope measurements combined with Iso-SPAC modeling are a promising tool that can be used to reproduce day-to-day variations in all surface energy balance components, as well as δ_{ET} and $\delta_{L,b}$. The measured and simulated results revealed that leaf development had a significant influence on day-to-day variations in δ_{ET} ($P<0.01$) but a small influence on $\delta_{L,b}$ ($P = 0.35$) at the canopy scale (Fig. 5).

The isotopic composition of soil evaporation, with its much-depleted isotope signature, showed a distinct pattern in the dual-isotope plots (Fig. S3). As shown in Fig. 7, the water was initially isotopically depleted in δ_{ET} during the initial growing season. Gradually, δ_{ET} lost its depleted signal with leaf development in the fast-growing season, accompanied by a rapid increase in T/ET, which led to increasingly enriched isotopic signals. There were smaller variations observed in δ_{ET} during the stable growing season. In a similar pattern, the initially isotopically enriched canopy leaf water lost its fractionation signal, leading to more depleted isotopic signals in the canopy leaf water, which may be explained by the increasing relative humidity in the canopy layer due to increasing amounts of water lost by transpiration (Wang et al. 2018a). Smaller variations in δ_{ET} were observed during the stable growing season. The results illustrated that canopy leaf water has well-behaved properties that were predictable for a multispecies grassland ecosystem at a daily time scale
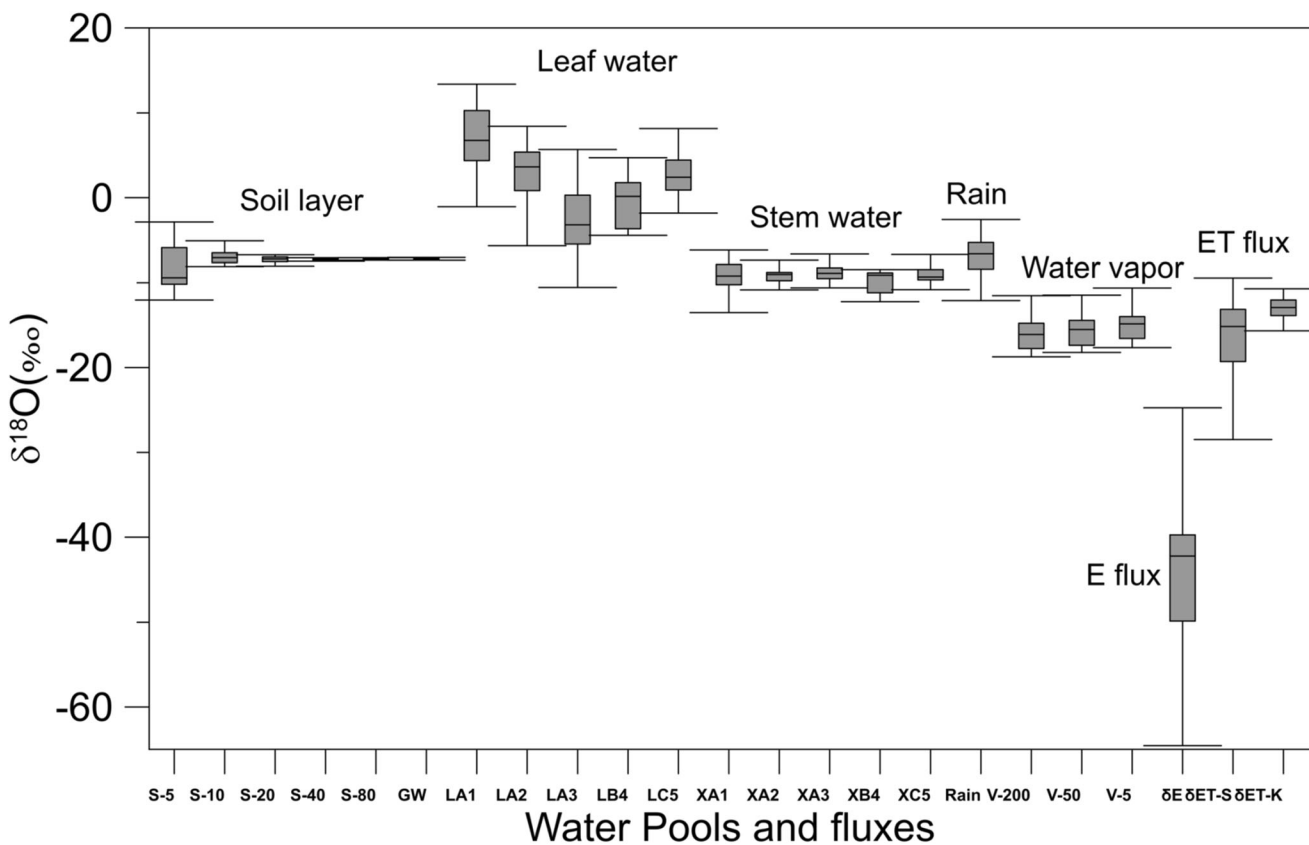
Fig. 6 Box-and-whisker plots showing the minimum, maximum, median, lower quartile, and upper quartile $\delta^{18}O$ values of soil water, groundwater, leaf water, and the stem water of the species *Miscanthus sinensis* measured from the top, middle, and base of the plants *(A)*, *Solidago altissima (B)*, and *Imperata cylindrical (C)*, rainwater, water vapor, the evapotranspiration fluxes estimated both by the Keeling plot approach (δET-K) and by the Iso-SPAC model (δET-S), and the soil evaporation flux (δE) simulated by the Iso-SPAC model. Here, S-5, S-10, S-20, S-40, and S-80 indicate soil water for species at depths of 5, 10, 20, 40, 60, and 80 cm, respectively. GW is groundwater; LA1, LA2,

and LA3 indicate leaf water for the species *Miscanthus sinensis* measured from the top, middle, and base, respectively; LB4 and LC5 denote leaf water collected from *Solidago altissima* and *Imperata cylindrical*, respectively; XA1, XA2, and XA3 indicate leaf water for the species *Miscanthus sinensis* measured from the top, middle, and base of the plant; XB4 and XC5 denote leaf water collected from *Solidago altissima* and *Imperata cylindrical*, respectively; and V-200, V-50, and V-5 indicate water vapor measured at the top (200 or 170 cm), middle (70 or 50 cm), and bottom (5 cm) levels, respectively

and emphasized that ecosystem properties (canopy-scale leaf water, ET flux) and behavior (seasonality) can be simulated and traced by many isotopic tracers (e.g., δ^2H and $\delta^{18}O$).

Implications of vegetation impacts on atmospheric moisture

Water vapor isotopes are used increasingly often to trace the impacts of vegetation on atmospheric moisture transport from regional to continental scales (e.g., Gat 1996; Yakir and Sternberg 2000). To quantify the impacts of the $\delta^{18}O$ values in ET, T, and E (δ_{ET}, δ_T, and δ_E) on the $\delta^{18}O$ value of atmospheric water vapor (δ_V), the ET, T, and E isoforcings, also called isofluxes (I_{ET}, I_T, and I_E), were defined as the products of ET, T, and E flux and the deviation of their isotopic ratios from that of near-surface atmospheric water vapor, respectively (Dansgaard 1953; Huang and Wen 2014). The formulas used to calculate I_{ET}, I_T, and I_E are given as follows:

$$I_{ET} = ET*(\delta_{ET}-\delta_V) \tag{1}$$

$$I_T = T*(\delta_T-\delta_V) \tag{2}$$

$$I_E = E*(\delta_E-\delta_V) \tag{3}$$

Combining online observations of δ_T or δ_{ET} with isotopic values of atmospheric vapor and land surface models can inform researchers on the interplay of water exchanges between vegetation or soils and the atmosphere (Wei et al. 2016). In a previous study, the local ET acted to increase the δD and $\delta^{18}O$ of δ_V, with isofluxes of 102.5 and 23.50 mmol m^{-2} s^{-1} ‰, respectively, in an agricultural ecosystem (Huang and Wen 2014) during the growing season. However, there are few processed-based modeling studies that have examined the impacts of vegetation on atmospheric moisture. Vegetation, through transpiration, impacts atmospheric moisture. The day-to-day variations in water fluxes (ET, T, and E) and
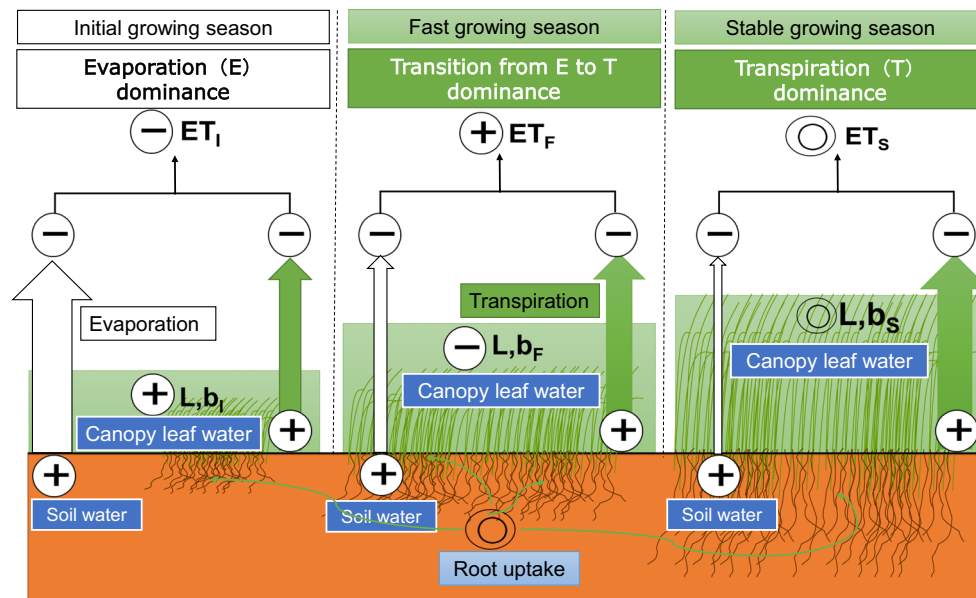
Fig. 7 Conceptualization of the processes affecting the water-stable isotopic compositions at the land–atmosphere interface during the growing season in a temperate grassland ecosystem. The plus symbol indicates an isotopic fractionation process leading to enrichment in heavy isotopes, the minus symbol represents depletion in heavy isotopes, and the zero symbol is a sign of a non-fractionating processes. The text indicates the labels of the closest arrows (up to two). The white arrows indicate evapotranspiration processes that are dominated by soil evaporation during the initial growing period (ET_I), and the green arrows indicate evapotranspiration processes that are dominated by plant transpiration during the fast-growing period (ET_F) and stable growing period (ET_S). The terms L,b_I, L,b_F, and L,b_S represent the canopy leaf water during the initial, fast, and stable growing periods, respectively

isofluxes (I_{ET}, I_T, and I_E) are shown in Fig. 8. The transpiration isoflux (I_T), which describes the isotopic imprint of transpiration on atmospheric vapor, always showed positive values ranging from 3.47 to 51.82 mm day^{-1} ‰, while the evaporation isoflux (I_E) was negative, ranging from −46.01 to−0.37 mm day^{-1} ‰ during the growing season. The results indicate that the δ_T values with enriched isotopic signatures (from −6.28 to −10.57‰) acted to increase the $\delta^{18}O$ of δ_V (from −11.22 to −19.59‰). In contrast, the δ_E values with depleted isotopic signatures (from −24.76 to −86.75‰) acted to decrease the $\delta^{18}O$ of δ_V (from −11.218 to −19.59‰). The I_{ET} added dynamic effects (from −40.37 to 38.19 mm day^{-1} ‰) on the $\delta^{18}O$ of δ_V, which depended on the seasonal tradeoff between I_T and I_E. I_{ET} acted to decrease the $\delta^{18}O$ of δ_V during the initial growing period and during the period after grass cutting when soil evaporation dominated the ET flux; I_{ET} also acted to increase the $\delta^{18}O$ of δ_V during the transpiration-dominated period. The impacts of vegetation on atmospheric moisture were also well captured by grass mowing in our study, which caused sensible heat flux and air temperature to increase while lET and relative humidity decreased (Fig. 1). The isotopic signals of the ET flux were also depleted due to increased soil evaporation (Fig. 4). The isotopic composition of the bulk leaf water increased because of the decrease in relative humidity (Fig. 4). The results obtained here emphasize that water fluxes and isotopic water flow paths (i.e., transpiration and evaporation) from temperate grasslands to the atmosphere are strongly controlled by the physiological properties of vegetation growth at a seasonal scale.
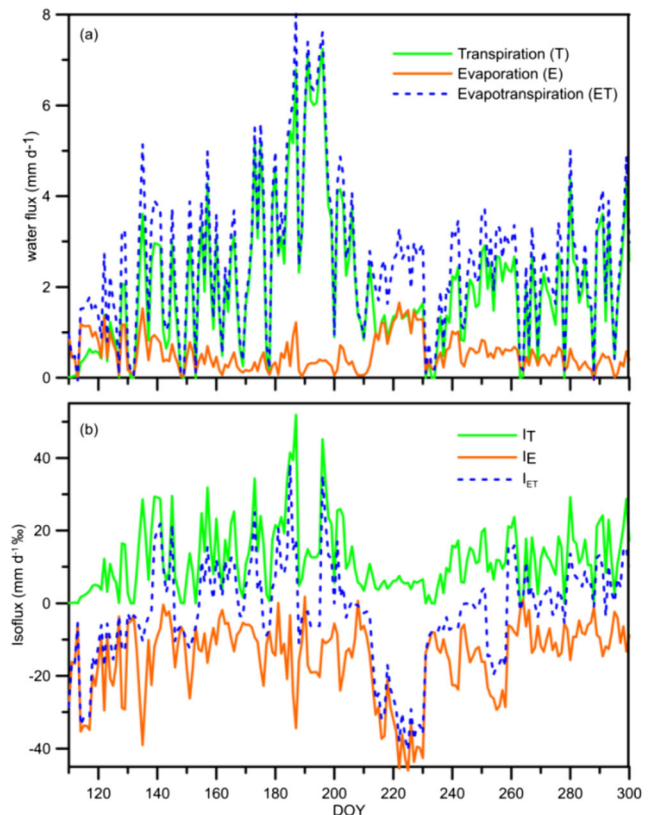

Fig. 8 Seasonal variations in (**a**) evapotranspiration, transpiration, and soil evaporation and (**b**) the evapotranspiration, transpiration, and soil evaporation isoforcings (I_{ET}, I_E, I_T) during the growing season

In this study, the water fluxes were partitioned into plant transpiration and soil evaporation to discuss their possible effects on atmospheric moisture. Nevertheless, Dubbert and Werner (2019) mentioned that there are still important open questions regarding how different plant functional types modulate water flows to the atmosphere. The results of our study support a general rule of thumb that water vapor from large water storage supplies (e.g., soil evaporation from large soil water pools) has abundant light isotope water supplies, which can support the continuous isotopic fractionation process, characterized by a slow turnover time with very depleted isotopic signatures that act to decrease δ_V. Water vapor from small water pools (e.g., grass leaves) has limited light isotope water supplies that can impair the isotopic fractionation process, characterized by a fast turnover time, and can reach ISS carrying the same isotopic signal as that of the original water plant uptakes (e.g., δ_X), which tends to increase the δ_V. Clearly, in the future, coupling different plant functional types with their water storages and turnover times to partition the water fluxes and couple the isotopic processes across multiple scales (e.g., from plot to regional scales) will be a promising way to improve our understanding of various vegetation feedbacks to climate systems that may buffer or enhance the susceptibility of these ecosystems.

Conclusions

In this study, in situ water isotopic measurements combined with process-based modeling were used to assess ecosystem water/energy flux partitioning, changes in the isotopic compositions of water fluxes (ET, soil evaporation, and transpiration), and canopy-scale leaf water enrichment as well as the relationships between water fluxes and vegetation growth during the growing season in a temperate grassland ecosystem. The seasonal changes in δ_{ET} could be explained well by a logarithmic function of the LAI. The day-to-day variations in T/ET and the proportion of latent heat flux to available energy could also be represented well by a logarithmic function of the LAI. These results demonstrate that leaf development controlled the isotopic seasonal variations in water fluxes by regulating the flux compositions. With the progress of leaf development, an increasing amount of water is lost by transpiration, leading to "cooling effects" and enhanced relative humidity at the canopy–atmosphere interface, which subsequently results in the decreased isotopic enrichment of canopy leaves. Transpiration/evaporation acted to increase/decrease the $\delta^{18}O$ of water vapor, and the local isoflux impacts on the $\delta^{18}O$ of water vapor were then determined by analyzing the seasonal tradeoffs between them. This study demonstrates the biotic controls on the day-to-day variations in water/energy flux partitioning using isotopic evidence at the canopy–atmosphere interface. It also reemphasizes that the isotope tracer approach is a useful tool for quantitative evaluations of the relationships among ecohydrological components in ecosystems.

References

Arora V (2002) Modeling vegetation as a dynamic component in soil-vegetation-atmosphere transfer schemes and hydrological models. Rev Geophys 40(2):1006. https://doi.org/10.1029/2001RG000103

Barbour MM, Roden JS, Farquhar GD, Ehleringer JR (2004) Expressing leaf water and cellulose oxygen isotope ratios as enrichment above source water reveals evidence of a Péclet effect. Oecologia 138(3): 426–435

Barbour MM, Schurr U, Henry BK, Wong SC, Farquhar GD (2000) Variation in the oxygen isotope ratio of phloem sap sucrose from castor bean. Evidence in support of the Péclet effect. Plant Physiol 123(2):671–680

Barnard RL, Salmon Y, Kodama N, Sorgel K, Holst J, Rennenberg H, Gessler A, Buchmann N (2007) Evaporative enrichment and time lags between $\delta^{18}O$ of leaf water and organic pools in a pine stand. Plant Cell Environ 30(5):539–550. https://doi.org/10.1111/j.1365-3040.2007.01654.x

Braud I, Bariac T, Gaudet JP, Vauclin M (2005) SiSPAT-Isotope, a coupled heat, water and stable isotope (HDO and $H_2^{18}O$) transport model for bare soil. Part I. Model description and first verifications. J Hydrol 309(1-4):277–300

Cernusak LA, Barbour MM, Arndt SK, Cheesman AW, English NB, Feild TS, Helliker BR, Holloway-Phillips MM, Holtum JAM, Kahmen A, McInerney FA, Munksgaard NC, Simonin KA, Song X, Stuart-Williams H, West JB, Farquhar GD (2016) Stable isotopes in leaf water of terrestrial plants. Plant Cell Environ 39:1081–1102. https://doi.org/10.1111/pce.12703

Cernusak LA, Arthur DJ, Pate JS, Farquhar GD (2003) Water relations link carbon and oxygen isotope discrimination to phloem sap sugar concentration in *Eucalyptus globulus*. Plant Physiol 131(4):1544–1554

Charney JG (1975) Dynamics of deserts and drought in the Sahel. Q J Roy Meteor Soc 101(428):193–202. https://doi.org/10.1002/qj.49710142802

Craig H, Gordon LI (1965) Deuterium and oxygen-18 variations in the ocean and the marine atmosphere. In: Proceedings of a conference on stable isotopes in oceanographic studies and palaeo temperatures. Spoleto Italy, pp 9–130

Cuntz M, Ogee J, Farquhar GD, Peylin P, Cernusak LA (2007) Modelling advection and diffusion of water isotopologues in leaves. Plant Cell Environ 30(8):892–909

Dansgaard W (1953) The abundance of ^{18}O in atmospheric water and water vapour. Tellus 5(4):461–469. https://doi.org/10.3402/tellusa. v5i4.8697

Dawson TE, Ehleringer JR (1993) Isotopic enrichment of water in the woody tissues of plants: implications for plant water source, water uptake, and other studies which use the stable isotopic composition of cellulose. Geochim Cosmochim Ac 57(14):3487–3492

Dickinson RE, Henderson-Sellers A (1988) Modeling tropical deforestation. Q J Roy Meteor Soc 114:439–462. https://doi.org/10.1002/qj. 49711448009

Dongmann G, Nürnberg HW, Förstel H, Wagener K (1974) On the enrichment of H_2^{18}O in the leaves of transpiring plants. Radiat Environ Biophys 11:41–52

Dubbert M, Cuntz M, Piayda A, Werner C (2014) Oxygen isotope signatures of transpired water vapor: the role of isotopic non-steady-state transpiration under natural conditions. New Phytol 203:1242–1252

Dubbert M, Werner C (2019) Water fluxes mediated by vegetation: emerging isotopic insights at the soil and atmosphere interfaces. New Phytol 221:1754–1763. https://doi.org/10.1111/nph.15547

Farquhar GD, Lloyd J, Taylor JA, Flanagan LB, Syvertsen JP, Hubick KT, Wong SC, Ehleringer JR (1993) Vegetation effects on the isotope composition of oxygen in atmospheric CO_2. Nature 363:439–443. https://doi.org/10.1038/363439a0

Farquhar GD, Cernusak LA (2005) On the isotopic composition of leaf water in the non-steady state. Funct Plant Biol 32(4):293–303

Fatichi S, Vivoni E, Ogden FL et al (2016) An overview of current applications, challenges, and future trends in distributed process-based models in hydrology. J Hydrol 537:45–60. https://doi.org/ 10.1016/j.jhydrol.2016.03.026

Flanagan LB, Bain JF, Ehleringer JR (1991) Stable oxygen and hydrogen isotope composition of leaf water in C3 and C4 plant species under field conditions. Oecologia 88(3):394–400

Griffis TJ (2013) Tracing the flow of carbon dioxide and water vapor between the biosphere and atmosphere: a review of optical isotope techniques and their application. Agric For Meteorol 174:85–109. https://doi.org/10.1016/j.agrformet.2013.02.009

Gat JR (1996) Oxygen and hydrogen isotopes in the hydrologic cycle. Annu Rev Earth Pl Sc 24(1):225–262. https://doi.org/10.1146/ annurev.earth.24.1.225

Good SP, Soderberg K, Guan KY, King EG, Scanlon TM, Caylor KK (2014) δ^2H isotopic flux partitioning of evapotranspiration over a grass field following a water pulse and subsequent dry down. Water Resour Res 50(2):1410–1432. https://doi.org/10.1002/ 2013WR014333

Good SP, Soderberg K, Wang LX, Caylor KK (2012) Uncertainties in the assessment of the isotopic composition of surface fluxes: a direct comparison of techniques using laser-based water vapor isotope analyzers. J Geophys Res 117:D15301. https://doi.org/10.1029/ 2011JD017168

Good SP, Noone D, Bowen G (2015) Hydrologic connectivity constrains partitioning of global terrestrial water fluxes. Science 349:175–177

Hammerle A, Haslwanter A, Tappeiner U, Cernusca A, Wohlfahrt G (2008) Leaf area controls on energy partitioning of a temperate mountain grassland. Biogeosciences 5(2):421–431

Helliker BR, Ehleringer JR (2000) Establishing a grassland signature in veins: ^{18}O in the leaf water of C3 and C4 grasses. P Natl Acad Sci USA 97(14):7894–7898. https://doi.org/10.1073/pnas.97.14.7894

Henderson-Sellers A, Fischer M, Aleinov I, McGuffie K, Riley W, Schmidt G, Sturm K, Yoshimura K, Irannejad P (2006) Stable water isotope simulation by current land-surface schemes: results of iPILPS phase 1. Glob Planet Chang 51(1-2):34–58

Hiyama T, Sugita M, Mikami M (1993) Comparisons of the latent heat fluxes evaluated by a weighing lysimeter and an energy balance method. Bull Environ Res Cent Univ Tsukuba 18:41–53

Hu ZM, Wen XF, Sun XM, Li LH, Yu GR, Lee XH, Li SG (2014) Partitioning of evapotranspiration through oxygen isotopic measurements of water pools and fluxes in a temperate grassland. J Geophys Res Biogeosci 119(3):358–371. https://doi.org/10.1002/ 2013JG002367

Hu ZM, Yu GR, Zhou YL, Sun X, Li Y, Shi P, Wang Y, Song X, Zheng Z, Zhang L, Li S (2009) Partitioning of evapotranspiration and its controls in four grassland ecosystems: application of a two-source model. Agric For Meteorol 149(9):1410–1420. https://doi.org/10. 1016/j.agrformet.2009.03.014

Huang LJ, Wen XF (2014) Temporal variations of atmospheric water vapor δD and δ^{18}O above an arid artificial oasis cropland in the Heihe River Basin. J Geophys Res-Atmos 119:11456–11476. https://doi.org/10.1002/2014JD021891

Jasechko S, Sharp ZD, Gibson JJ, Birks SJ, Yi Y, Fawcett PJ (2013) Terrestrial water fluxes dominated by transpiration. Nature 496: 347–350. https://doi.org/10.1038/nature11983

Jelka BB, Christian M, Alexander K (2019) Eddy covariance measurements of the dual-isotope composition of evapotranspiration. Agric For Meteorol 269-270:203–219. https://doi.org/10.1016/j. agrformet.2019.01.035

Kahmen A, Simonin K, Tu KP, Merchant A, Callister A, Siegwolf R, Dawson TE, Arndt SK (2008) Effects of environmental parameters, leaf physiological properties and leaf water relations on leaf water δ^{18}O enrichment in different Eucalyptus species. Plant Cell Environ 31:738–751

Keeling CD (1958) The concentration and isotopic abundances of atmospheric carbon dioxide in rural areas. Geochim Cosmochim Ac 13(4):322–334

Lai CT, Ehleringer JR, Bond BJ, Paw KT (2005) Contributions of evaporation, isotopic non-steady state transpiration and atmospheric mixing on the δ^{18}O of water vapor in Pacific Northwest coniferous forests. Plant Cell Environ 29:77–94

Lean J, Rowntree PR (1997) Understanding the sensitivity of a GCM simulation of Amazonian deforestation to the specification of vegetation and soil characteristics. J Clim 10:1216–1235

Leaney FW, Osmond CB, Allison GB, Ziegler H (1985) Hydrogen-isotope composition of leaf water in C_3 and C_4 plants: its relationship to the hydrogen-isotope composition of dry matter. Planta 164: 215–220

Lee XH, Sargent S, Smith R, Tanner B (2005) In-situ measurement of the water vapor 18O/16O isotope ratio for atmospheric and ecological applications. J Atmos Ocean Technol 22:555–565

Lee X, Kim K, Smith R (2007) Temporal variations of the O-18/O-16 signal of the whole-canopy transpiration in a temperate forest. Global Biogeochem Cy 21:3013

Lee XH, Griffis TJ, Baker JM, Billmark KA, Kim K, Welp LR (2009) Canopy-scale kinetic fractionation of atmospheric carbon dioxide and water vapor isotopes. Global Biogeochem Cy 23:GB1002. https://doi.org/10.1029/2008GB003331

Lian X, Piao SL, Chris H et al (2018) Partitioning global land evapotranspiration using CMIP5 models constrained by observations. Nat Clim Chang 8(7):640–646. https://doi.org/10.1038/s41558-018-0207-9

Li SG, Lai CT, Lee G, Shimoda S, Yokoyama T, Higuchi A, Oikawa T (2005) Evapotranspiration from a wet temperate grassland and its sensitivity to micro environmental variables. Hydrol Process 19(2): 517–532. https://doi.org/10.1002/hyp.5673

Ma WC, Asanuma J, Xu JQ, Onda Y (2018) A database of water and heat observations over grassland in the north-east of Japan. Earth Syst Sci Data 10(4):2295–2309. https://doi.org/10.5194/essd-10-2295-2018

Maxwell RM, Condon LE (2016) Connections between groundwater flow and transpiration partitioning. Science 353:377–380. https://doi.org/10.1126/science.aaf7891

Moreira M, Sternberg L, Martinelli L, Victoria R, Barbosa E, Bonates L, Nepstad D (1997) Contribution of transpiration to forest ambient vapor based on isotopic measurements. Glob Chang Biol 3(5):439–450. https://doi.org/10.1046/j.1365-2486.1997.00082.x

Riley WJ, Still CJ, Torn MS, Berry JA (2002) A mechanistic model of $H_2^{18}O$ and $C^{18}OO$ fluxes between ecosystems and the atmosphere: model description and sensitivity analyses. Global Biogeochem Cy 16(4):1095–42-14. https://doi.org/10.1029/2002GB001878

Song X, Loucos KE, Simonin KA, Farquhar GD, Barbour MM (2015) Measurements of transpiration isotopologues and leaf water to assess enrichment models in cotton. New Phytol 206(2):637–646. https://doi.org/10.1111/nph.13296

Sprenger M, Leistert H, Gimbel K, Weiler M (2016) Illuminating hydrological processes at the soil-vegetation-atmosphere interface with water stable isotopes. Rev Geophys 54:674–704

Twine TE, Kustas WP, Norman JM, Cook DR, Houser PR, Meyers TP, Prueger JH, Starks PJ, Wesely ML (2000) Correcting eddy-covariance flux underestimates over a grassland. Agric For Meteorol 103(3):279–300. https://doi.org/10.1016/S0168-1923(00)00123-4

Wang P, Yamanaka T (2014) Application of a two-source model for partitioning evapotranspiration and assessing its controls in temperate grasslands in central Japan. Ecohydrology 7:345–353. https://doi.org/10.1002/eco.1352

Wang P, Yamanaka T, Li XY, Wei ZW (2015) Partitioning evapotranspiration in a temperate grassland ecosystem: numerical modeling with isotopic tracers. Agric For Meteorol 208:16–31. https://doi.org/10.1016/j.agrformet.2015.04.006

Wang P, Yamanaka T, Li XY, Wu XC, Chen B, Liu YP, Wei ZW, Ma WC (2018a) A multiple time scale modeling investigation of leaf water isotope enrichment in a temperate grassland ecosystem. Ecol Res 33(5):901–915. https://doi.org/10.1007/s11284-018-1591-3

Wang P, Li XY, Huang YM, Liu SM, Xu ZW, Wu XC, Ma YJ (2016) Numerical modeling the isotopic composition of evapotranspiration in an arid artificial oasis cropland ecosystem with high–frequency water vapor isotope measurement. Agric For Meteorol 230–231:79–88

Wang P, Li XY, Wang LX, Wu XC, Hu X, Fan Y, Tong YQ (2018b) Divergent evapotranspiration partition dynamics between shrubs and grasses in a shrub-encroached steppe ecosystem. New Phytol 219(4):1325–1337. https://doi.org/10.1111/nph.15237

Wang LX, Caylor KK, Villegas JC, Barron-Gafford GA, Breshears DD, Huxman TE (2010) Partitioning evapotranspiration across gradients of woody plant cover: assessment of a stable isotope technique. Geophys Res Lett 37(9). https://doi.org/10.1029/2010GL043228

Wang LX, Good SP, Caylor KK (2014) Global synthesis of vegetation control on evapotranspiration partitioning. Geophys Res Lett 41(19):6753–6757

Wei ZW, Yoshimura K, Okazaki A, Kim W, Liu ZF, Yokoi M (2015) Partitioning of evapotranspiration using high-frequency water vapor isotopic measurement over a rice paddy field. Water Resour Res 51:3716–3729. https://doi.org/10.1002/2014WR016737

Wei ZW, Yoshimura K, Okazaki A, Ono K, Kim W, Yokoi M, Lai CT (2016) Understanding the variability of water isotopologues in near-surface atmospheric moisture over a humid subtropical rice paddy in Tsukuba, Japan. J Hydrol 533:91–102. https://doi.org/10.1016/j.jhydrol.2015.11.044

Wei ZW, Yoshimura K, Wang LX, Miralles DG, Jasechko S, Lee XH (2017) Revisiting the contribution of transpiration to global terrestrial evapotranspiration. Geophys Res Lett 44:2792–2801. https://doi.org/10.1002/2016GL072235

Wei ZW, Lee XH, Wen XF, Xiao W (2018a) Evapotranspiration partitioning for three agro-ecosystems with contrasting moisture conditions: a comparison of an isotope method and a two-source model calculation. Agric For Meteorol 252:296–310

Wei ZW, Lee XH, Patton EG (2018b) ISOLESC: A coupled isotope-LSM-LES-cloud modeling system to investigate the water budget in the atmospheric boundary layer. J Adv Model Earth Sy 10(10):2589–2617. https://doi.org/10.1029/2018MS001381

Wen X-F, Sun X-M, Zhang S-C, Yu G, Sargent SD, Lee X (2008) Continuous measurement of water vapor D/H and 18O/16O isotope ratios in the atmosphere. J Hydrol 349(3–4):489–500

Wen X-F, Yang B, Sun X-M, Lee X (2016) Evapotranspiration partitioning through in-situ oxygen isotope measurements in an oasis cropland. Agric and For Meteorol 230–231:89–96

West AG, Patrickson SJ, Ehleringer JR (2006) Water extraction times for plant and soil materials used in stale isotope analysis. Rapid Commun Mass Sp 20:1317–1321. https://doi.org/10.1002/rcm.2456

Williams D, Cable W, Hultine K, Hoedjes J, Yepez E, Simonneaux V, Er-Raki S, Boulet G, De Bruin H, Chehbouni A (2004) Evapotranspiration components determined by stable isotope, sap flow and eddy covariance techniques. Agric and For Meteorol 125(3–4):241–258

Willmott CJ, Ackleson SG, Davis RE, Feddema JJ, Klink KM, Legates DR, O'donnell J, Rowe CM (1985) Statistics for the evaluation and comparison of models. J Geophys Res 90(C5):8995

Wilson K, Goldstein A, Falge E, Aubinet M, Baldocchi D, Berbigier P, Bernhofer C, Ceulemans R, Dolman H, Field C, Grelle A, Ibrom A, Law BE, Kowalski A, Meyers T, Moncrieff J, Monson R, Oechel W, Tenhunen J, Valentini R, Verma S (2002) Energy balance closure at FLUXNET sites. Agric For Meteorol 113(1-4):223–243. https://doi.org/10.1016/S0168-1923(02)00109-0

Xiao W, Lee XH, Wen XF, Sun XM, Zhang SC (2012) Modeling biophysical controls on canopy foliage water ^{18}O enrichment in wheat and corn. Glob Chang Biol 18:1769–1780

Xiao W, Lee XH, Griffis TJ, Kim K, Welp LR, Yu Q (2010) A modeling investigation of canopy-air oxygen isotopic exchange of water vapor and carbon dioxide in a soybean field. J Geophys Res 115(G1):G01004. https://doi.org/10.1029/2009JG001163

Xiao W, Wei ZW, Wen XF (2018) Evapotranspiration partitioning at the ecosystem scale using the stable isotope method-a review. Agric For Meteorol 263:346–361. https://doi.org/10.1016/j.agrformet.2018.09.005

Yakir D, Sternberg LSL (2000) The use of stable isotopes to study ecosystem gas exchange. Oecologia 123(3):297–311. https://doi.org/10.1007/s004420051016

Yakir D, Wang XF (1996) Fluxes of CO_2 and water between terrestrial vegetation and the atmosphere estimated from isotope measurements. Nature 380:515–517 https://www.researchgate.net/publication/232786872

Yamanaka T, Tsunakawa A (2007) Isotopic signature of evapotranspiration flux and its use for partitioning evaporation/transpiration components. Tsukuba Geoenviron Sci Univ Tsukuba 3:11–21

Yamanaka T, Onda Y (2011) On measurement accuracy of liquid water isotope analyzer based on wavelength-scanned cavity ring-down spectroscopy (WS-CRDS). Bull Terrestrial Environ Res Cent Univ Tsukuba 12:31–40

Yepez EA, Williams DG, Scott RL, Lin GH (2003) Partitioning overstory and understory evapotranspiration in a semiarid savanna woodland from the isotopic composition of water vapor. Agric For Meteorol 119(1-2):53–68. https://doi.org/10.1016/S0168-1923(03)00116-3

Yoshimura K, Miyazaki S, Kanae S, Oki T (2006) Iso-MATSIRO, a land surface model that incorporates stable water isotopes. Glob Planet

Chang 51(1):90–107. https://doi.org/10.1016/j.gloplacha.2005.12.007

Zhao P, Zhang XT, Li S, Kang SZ (2017) Vineyard energy partitioning between canopy and soil surface: dynamics and biophysical controls. J Hydrometeorol 18(7):1809–1829

Zhou GY, Wei XH, Chen XZ, Zhou P, Liu X, Xiao Y, Sun G, Scott DF, Zhou S, Han L, Su Y (2015) Global pattern for the effect of climate and land cover on water yield. Nat Commun 6:5918

Zhao P, Tang XY, Zhao P, Wang C, Tang JL (2013) Identifying the water source for subsurface flow with deuterium and oxygen-18 isotopes of soil water collected from tension lysimeters and cores. J Hydrol 503(30):1–10